Available online at www.sciencedirect.com
ScienceDirect
Applied Surface Science 253 (2007) 5196–5202
applied surface science
www.elsevier.com/locate/apsusc

Surface analysis of the nanostructured W–Ti thin film deposited on silicon

S. Petrović [a,*], N. Bundaleski [a], D. Peruško [a], M. Radović [a], J. Kovač [b], M. Mitrić [a], B. Gaković [a], Z. Rakočević [a]

[a] *Institute of Nuclear Sciences – Vinča, P.O. Box 522, 11001 Belgrade, Serbia*
[b] *"Jožef Stefan" Institute, Jamova 39, 1000 Ljubljana, Slovenia*

Received 24 February 2006; received in revised form 30 October 2006; accepted 30 October 2006
Available online 17 December 2006

Abstract

The W–Ti thin films are deposited by the dc Ar^+ sputtering of W(70%)–Ti(30%) a.t. target on silicon substrates. The surface composition and structure of the thin film, previously exposed to air, was carried out. The surface structure was undertaken using grazing incidence X-ray diffraction (GIXRD), and compared to that of the thin film interior. The surface morphology was determined by the Scanning Tunneling Microscopy (STM). The surface composition and chemical bonding of elements on the Ti–W film were analyzed by X-ray photoelectron spectroscopy (XPS) and Low Energy Ion Scattering (LEIS). The measurements show that the overlayer of metallic oxides TiO_2 and WO_3 is formed. The first atomic layer is occupied by TiO_2 only, and its thickness is estimated to about 3.2 ± 0.4 nm. The strong surface segregation of Ti is triggered by the surface oxidation, which is confirmed by the thermodynamical considerations.

Keywords: W–Ti thin films; Surface segregation; GIXRD; STM; XPS; LEIS

1. Introduction

It is well known that W–Ti thin films suppress the interdiffusion between metal contact structures on silicon [1]. The most frequently used stoichiometry is 70:30 W:Ti a. t., where tungsten serves as the diffusion barrier (atomic diffusivities of most metals in tungsten is low) and titanium prevents grain boundary diffusion. The addition of titanium to tungsten also improves the corrosion resistance and the adhesive strength of the barrier [1,2]. Hence, their additional properties, such as thermomechanical stability, low electromigration and high corrosion resistance, make these films convenient as interdiffusion barriers for metallic contacts of semiconductor devices, especially in the case of high current densities and at increased temperatures [3].

The most probable diffusion mechanism through the barrier layers is the grain boundary diffusion, which is higher than the volume diffusion by orders of magnitude. For this reason, special attention has been given to the microstructure and to the concentration of impurities in the diffusion barrier layers, which govern grain boundary diffusion [4]. The addition of nitrogen and/or oxygen to the argon sputtering gas during the magnetron deposition of W–Ti thin film lowers the diffusion coefficient of a contact metal. The possible explanation of this effect is that the introduced gas atoms are collected at defect sites and grain boundaries, which contributes to blocking the open diffusion paths [1].

Different multilayered metal structures obtained by ion sputtering with W–Ti as a diffusion barrier layer has been investigated in [4]. The improvement of the diffusion barrier properties was achieved by exposing samples to air deliberately after the W–Ti deposition in order to contaminate them with oxygen [5]. According to the Auger Electron Spectroscopy (AES) depth profiling of the multilayered metal structures previously exposed to air, the concentration increase of O and Ti and decrease of W concentration took place. While the increase of the oxygen concentration on the mentioned interface is expected, the change of the Ti and W interface concentrations with respect to the thin film interior cannot be explained straightforwardly. Moreover, several questions arise

* Corresponding author.
E-mail address: spetro@vin.bg.ac.yu (S. Petrović).

0169-4332/$ – see front matter © 2007 Elsevier B.V. All rights reserved.
doi:10.1016/j.apsusc.2006.10.077

about the structure, composition and topography of the W–Ti surface formed in this way, since it becomes a substrate for the deposition of metallic contacts.

Surface structure and composition of W–Ti thin film deposited by dc sputtering is analyzed in this work. The samples were exposed to the air after the deposition, i.e. before the analyses. This contributed, as it will be shown, to significant changes of the surface composition and provided important information concerning the oxygen interaction with W–Ti thin film at room temperature. The crystal structure of W–Ti thin films was analyzed by X-ray diffraction (XRD) using both, the standard geometry and grazing incidence in order to resolve the structure of the surface region from those of the thin film interior and the sample substrate. The surface morphology and the size of the surface agglomerates were determined using the Scanning Tunneling Microscopy (STM). The surface composition has been determined using X-ray photoelectron spectroscopy (XPS), as well as Low Energy Ion Scattering (LEIS). LEIS and XPS are complementary techniques for the surface analysis: XPS provides both the surface composition analysis and the chemical information, while the LEIS information depth is restricted to the first few atomic layers (which makes this technique particularly suitable for investigating the surface segregation phenomena). The composition of the thin film interior has been also determined, using XPS together with the Ar^+ ion sputtering.

2. Experimental

Thin films of W–Ti were deposited by dc sputtering (in Balzers Sputtron II system) of W:Ti 70:30 a. t. % target. The used substrates were (100) n-Si wafers, cleaned in an HF solution and in de-ionized water before mounting in the chamber. Before deposition, the sputtering chamber was evacuated by a turbomolecular pump, down to a final pressure 1×10^{-3} Pa. The substrate surfaces were cleaned by bias sputtering. The cleaning procedure included Ar^+ bombardment of substrates during 2 min at $I = 50$ mA and $V = 1$ kV. The sputtering deposition was performed at room temperature and the partial pressure of argon 1×10^{-1} Pa. Under such conditions, the deposition rate was approximately 0.095 nm s^{-1}. The thickness of deposited WTi thin films is 105 nm, measured by Talystep. After the deposition, the samples have been exposed to air at room temperature and relative humidity of about 50% for 10 days. We assume that equilibrium state at the sample surface was achieved during this period. The samples were then analyzed by different techniques.

The phase composition and crystalline structure of W–Ti thin films was recorded by grazing incidence X-ray diffraction. Cu Kα X-ray diffraction patterns were collected by a Bruker D8 Advance Diffractometer with parallel beam optics. The beam optics was adjusted by a parabolic Gobel mirror (push plug Ni/C) with horizontal grazing incidence soller slit of 0.120 and LiF monochromator. Angle 2θ in the range 30°–80° were scanned by a step of 0.02 degree in time sequence of 1 s.

The surface morphology of deposited W–Ti layer was analyzed by the STM NANOSCOPE III at room temperature and under atmospheric pressure. The STM image was obtained in constant current mode using a Pt(10%)Ir tunneling tip. Agglomerate size and mean surface roughness of the deposited W–Ti thin film were measured using the section analysis program in STM.

The W–Ti thin film was analyzed by XPS in the PHI XPS-TFA spectrometer. Monochromatized Al Kα X-ray beam was used for analysis of as-received surface and during the XPS depth profiling. The survey spectra and narrow scan spectra of Ti 2p, W 4f and O 1s were taken at resolutions of about 2.0 and 0.9 eV, respectively. The depth profile of the W–Ti film was obtained by ion bombardment of sample surface with 3 keV Ar^+ ions. A take-off angle of photoelectrons was 45° with respect to the sample surface. Concentrations of elements were calculated from peak areas using sensitivity factors provided by the instrument manufacturer.

LEIS experiments were carried out using the setup described in detail elsewhere [6]. He^+, Ne^+ and Ar^+ ions generated in a discharge-type ion source were accelerated to the desired energy in the range from 500 to 2000 eV, mass analyzed and focused onto the target inside the UHV sample chamber. The energy spread of the primary ion beam does not exceed few eV. Typical ion current density during the measurements was about 1 μA/cm^2. The scattered ions were energy analyzed using a 127° cylindrical electrostatic energy analyzer of 120 mm radius and a resolving power of about 140 FWHM. The incoming angle ψ and scattering angle θ can be continuously changed in the range from 0° to 90°. In all LEIS experiments specular geometry ($\theta = 2\psi$) was employed. The analyzed ions were post-accelerated in order to avoid the detection sensitivity dependence on the energy of detected ions. The sample has been cleaned by grazing incidence sputtering with He^+ ions with the current density of about 3 μA/cm^2 until the steady state was obtained. This way of surface cleaning was chosen in order to suppress the problem with the surface composition change during the standard cleaning procedure (which consists of heavy ion sputtering and sample heating cycles). During the experiment, the pressure in the chamber was lower then 5×10^{-7} Pa.

3. Results

3.1. XRD analysis

X-ray diffraction was used to reveal phase composition and crystal structure of the samples. Fig. 1(a) represents XRD spectrum of the 105 nm thick W–Ti film. In the presented spectrum two wide peaks can be observed: the first at about $2\theta = 40°$ of relatively low intensity and the second positioned at $2\theta = 70°$, which is more intense. Tungsten has a body centered cubic structure with a lattice parameter $a = 3.1648$ Å. The low intensity peak is attributed to W (1 1 0) plane situated at $2\theta = 40.264°$ (JCPDS card 04-0806). On the other hand, the lattice parameter calculated from the exact position of the mentioned peak amounts $a = 3.2237$ Å. The discrepancy between the measured lattice parameter and the value obtained in the referent measurements is due to the formation of the

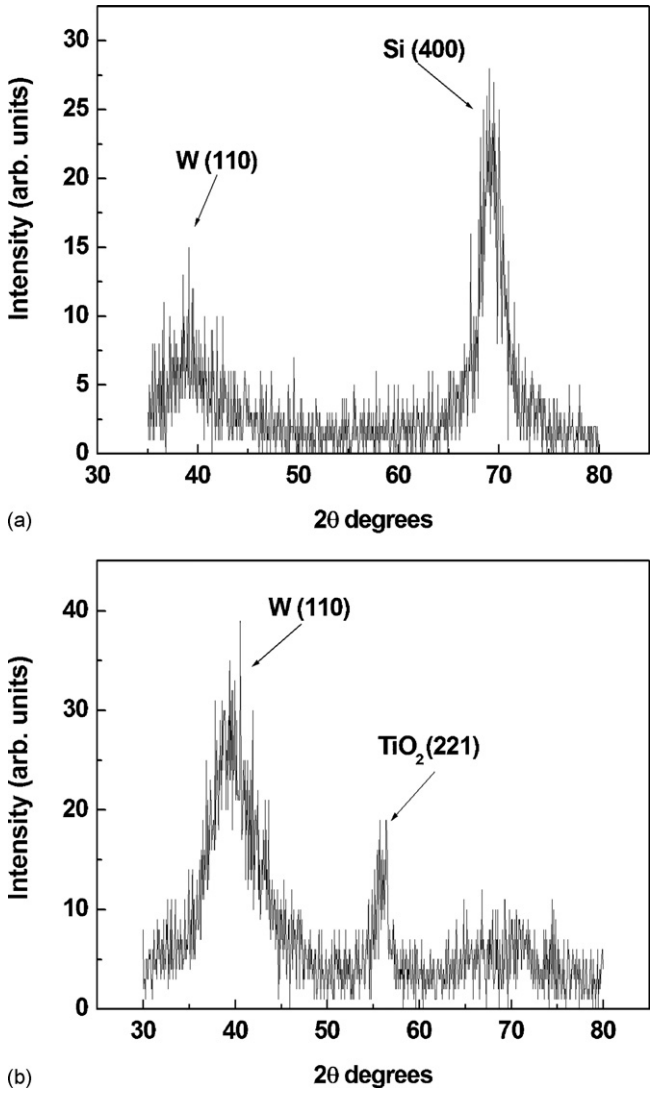

Fig. 1. XRD diffractograms of W–Ti films deposited on silicon: (a) standard geometry and (b) incident angle of 3° (GIXRD).

titanium solid solution in a tungsten matrix—the presence of titanium in the tungsten lattice contributes to its expansion [7,8]. The mean grain size of W–Ti thin film was estimated to about 7.1 nm by the analysis of the tungsten peak width. The second peak in the XRD spectrum is attributed to the Si phase with (4 0 0) orientation at the position $2\theta = 69.704^\circ$ (JCPDS card 35-241). The intensity of this peak decreases with the film thickness and disappears for 400 nm thick thin films due to the limited information depth of XRD [9].

Grazing incidence X-ray diffraction (GIXRD) is an effective technique to characterize a near surface region. The XRD spectrum of the W–Ti deposit measured for the 3° incident angle is shown in Fig. 1(b). The great qualitative difference between this spectrum and the previous one is obvious, indicating different phase composition of the thin film as compared to its near surface region. The peak corresponding to the Si substrate is not present in diffractogram due to the decreased information depth of GIXRD as compared to XRD. On the other hand, the peak corresponding to W (1 1 0)

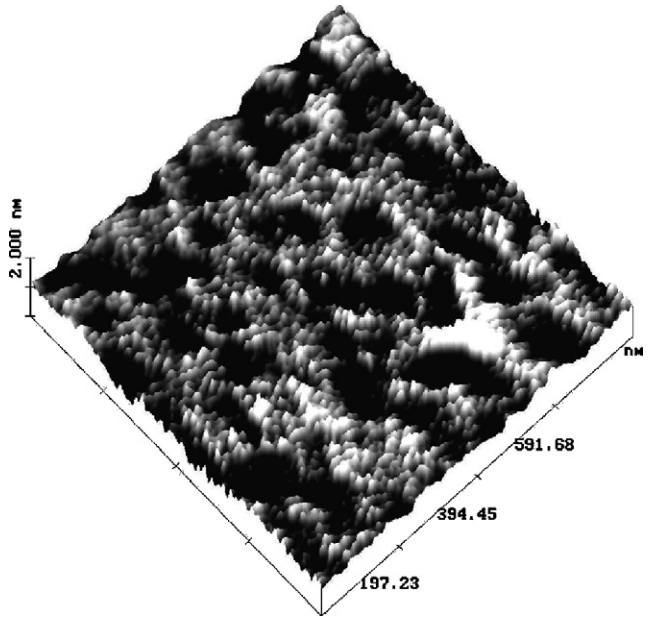

Fig. 2. STM image of the 105 nm thick W–Ti thin film surface.

becomes dominant and another peak at about $2\theta = 56^\circ$ is observed. The additional peak can be attributed to the TiO_2 (2 2 1) plane situated at position $2\theta = 55.854^\circ$ (JCPDS card 21-1236).

3.2. STM

The surface morphology of W–Ti thin film deposited on Si substrate can be seen from the STM microphotographs, presented in Fig. 2. The lateral dimension of the grains at the W–Ti thin film surface was estimated to about 32 nm. The deposited material covers the Si substrate approximately uniformly. The initial surface roughness of Si substrate is about 0.5 nm, while the mean surface roughness of deposited W–Ti film is about 0.57 nm. The difference between the initial surface roughness of Si substrate and that of the W–Ti film does not exceed the experimental error, meaning that the formed thin film follows the morphology of the substrate.

3.3. XPS results

The XPS survey spectrum of the W–Ti thin film surface is presented in Fig. 3. The peaks corresponding to Ti 2p, W (4p, 4d, 4f) and O 1s core levels are present in the spectrum, as well as two peaks of impurities (C 1s and N 1s) adsorbed at the surface. The surface atomic concentrations of W, Ti, O, N and C at the surface are 13%, 8%, 37%, 1% and 41%, respectively (homogeneous in-depth composition in subsurface region is assumed). We should note that the surface sensitivity of the XPS method, i.e. the depth from which photoelectrons contribute to XPS signals is between 1 and 3 nm for our geometry. The Ti 2p and W 4f spectra are presented in Fig. 4. By the analysis of the chemical shifts, the chemical bonds were determined: titanium is present at the surface as TiO_2 (at the

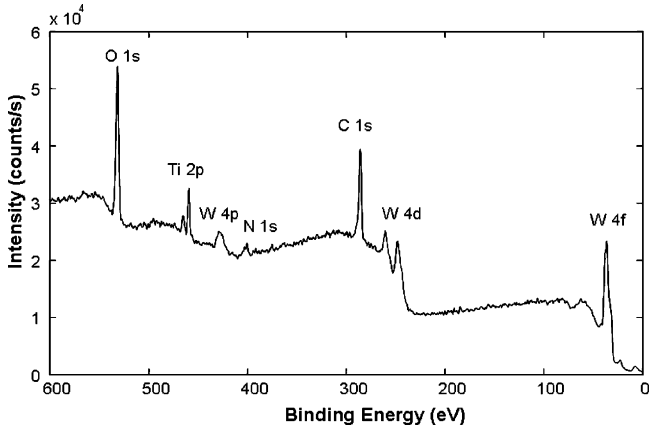

Fig. 3. XPS survey spectrum of the surface of the W–Ti film exposed to air.

binding energy E_b = 459.2 eV, Fig. 4a), while both, the metallic tungsten (E_b = 31.5 eV) and the oxidized tungsten phase WO_3 (E_b = 36.1 eV) can be observed in Fig. 4b [10]. The W 4f spectra versus the sputtering time are presented in Fig. 5. While the WO_3 phase dominates in the surface region, the W inside the thin film is in the metallic phase only. Hence, we conclude that the W–Ti film is covered by the mix of TiO_2 and WO_3.

The composition of the thin film interior significantly differs from that of the surface, and the steady state was obtained at the depth of about 7 nm. The relative concentrations of W, Ti and O inside the thin film were 77%, 8% and 15%, respectively, while

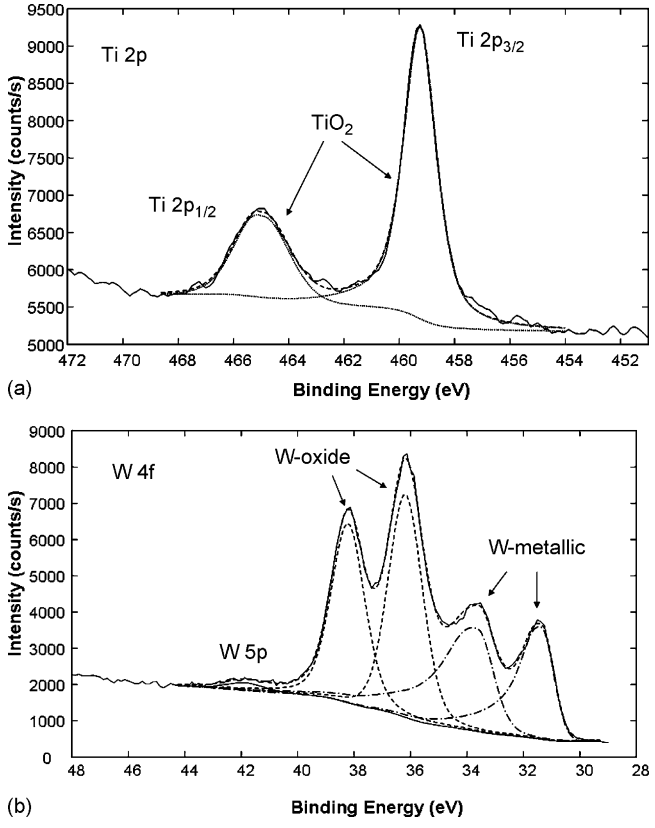

Fig. 4. XPS narrow scan spectra of (a) Ti 2p and (b) W 4f regions obtained on the surface of the W–Ti film after air exposure. The curve fitted components in the XPS spectra present different Ti and W chemical species.

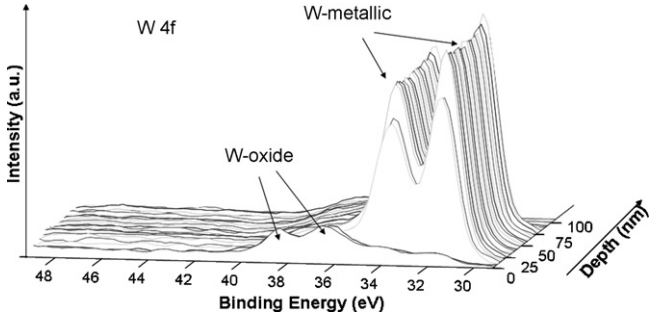

Fig. 5. XPS spectra of W 4f as a function of sputtered depth obtained during XPS depth profiling of the W–Ti film.

the presence of nitrogen and carbon was not detected. Consequently, the Ti concentration is approximately the same at the surface and inside the film, while W is depleted in the surface region. The thickness d of the TiO_2 layer over the W–Ti film can be estimated by attenuation of the W 4f metallic peak measured at the surface ($I_{W\text{-met,S}}$) with respect to that from the film interior ($I_{W\text{-met,F}}$), using the expression [10]:

$$\frac{I_{W\text{-met,S}}}{I_{W\text{-met,F}}} = \exp\left(-\frac{d}{\lambda_{W,TiO_2}\sin(\theta)}\right) \quad (1)$$

where λ_{W,TiO_2} is the attenuation length of W 4f photoelectrons in the TiO_2 layer and θ is the take-off angle of photoelectrons with respect to the sample surface. Using a value of 2.2 nm for λ_{W,TiO_2} [11], the estimated thickness of the TiO_2 layer is 3.2 ± 0.4 nm.

3.4. LEIS measurements

The spectrum of He^+ ions scattered from the W–Ti thin film surface is presented in Fig. 6. The primary ion energy was 2 keV and the scattering angle was 90°. Obviously, the three peaks present in the spectrum can be contributed to the He^+ ions singly scattered from oxygen, titanium and tungsten. Both,

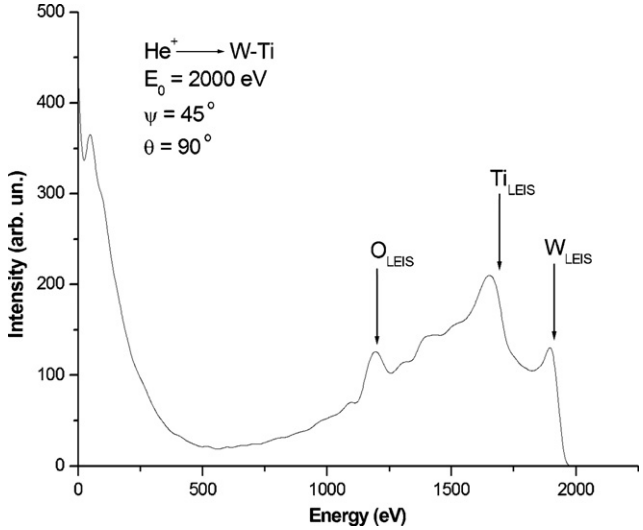

Fig. 6. LEIS spectrum of 2 keV He^+ ions scattered to 90° from the W–Ti thin film surface.

tungsten and titanium peaks have intense low energy tails due to the reionization effects often present in the case of He^+ scattering from transition metals [12]. The reionization effects are further increased due to the presence of oxygen [13], which significantly hardens the quantitative analysis: single scattering peaks lie on the baseline which represents a superposition of the titanium and tungsten low energy tails. In spite of the difficulties concerning the determination of the peak intensities, it can be said that the titanium peak intensity is the greatest while that of oxygen has the lowest intensity. Peak intensity in LEIS spectra I_S is proportional to the surface concentration of atomic species n_S, scattering cross-section during the binary collision σ_S and the ion surviving probability during the single elastic collision P^+: $I_S \sim n_S \sigma_S P^+$. The scattering cross-sections for 2 keV He^+ projectiles scattered from oxygen, titanium and tungsten ($\theta = 90^\circ$) are calculated using the ZBL interaction potential [14]. The ratio is the following: $\sigma_W:\sigma_{Ti}:\sigma_O = 12:3.2:1$. Although getting reliable information concerning the ion surviving probability is difficult, a rough estimation can be made. In the case of He^+ projectiles a correlation was found between P^+ and the electronic structure of target atoms: the ion surviving probability decreases with increasing the number of filled d-states [15]. According to this, the He^+ ion surviving probability should be lower for titanium than for tungsten. As the scattering cross-section and the ion surviving probability of tungsten are both greater as compared to those of titanium, we conclude that the tungsten surface concentration is lower as compared to that of the titanium.

The surface specificity of the LEIS technique can be increased by increasing the projectile atomic number and by decreasing the primary energy: both parameters increase scattering cross-sections. The decrease of the primary energy also decreases the ion survival probability, which contributes to the more efficient neutralization of the projectiles scattered from deeper atomic layers and further increases the surface sensitivity. Hence, LEIS experiments has been performed using Ne^+ and Ar^+ projectiles as well, in order to get a better insight into the composition of the first atomic layer. Since the data available for the ion surviving probabilities in the case of Ne^+ and especially of Ar^+ are poor, the quantitative estimations of the following spectra are even harder. The spectra of Ne^+ and Ar^+ scattered to greater angles ($\theta = 90^\circ$ for instance) did not give any new information because the single scattering peaks were overlapped by the very intense secondary ion spectrum. The intense secondary ion emission yield can be explained by the presence of oxygen at the surface (this well known effect is employed in commercial SIMS systems for increasing the yield of positive secondary ions). Consequently, the spectra were measured for smaller scattering and outgoing angles in order to suppress the problem with secondary ions. This geometry enabled to see direct recoiled peaks (DR), as well [16]. Moreover, the decrease of the scattering angle further increased the scattering cross-section and consequently, increases the surface sensitivity. As the obtained spectra were not influenced by the ion fluence, it can be concluded that the preferential sputtering effects did not take place in these measurements. The energy spectra of Ne^+ ions scattered from the W–Ti thin film are presented in Fig. 7. The spectra are normalized to the same intensity. In the case of 1 keV ion scattering, a DR oxygen peak is obtained. The broad maximum obtained in experiment with 2 keV ions is most likely a superposition of LEIS and DR oxygen peaks. Tungsten peak is clearly visible only for primary ion energy of 2 keV, while it becomes very small in the 1 keV Ne^+ spectrum. This fact confirms the surface segregation of titanium.

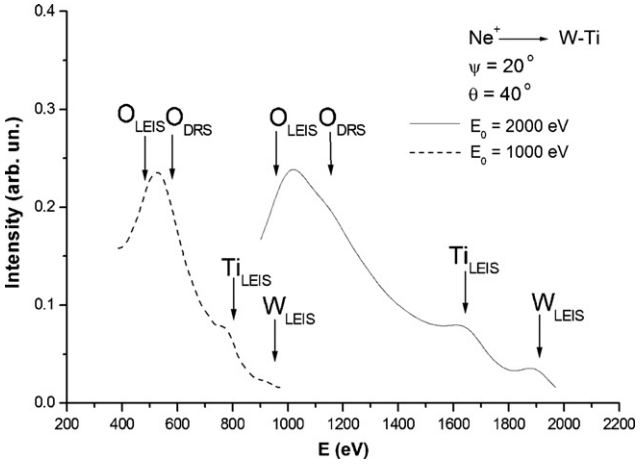

Fig. 7. LEIS spectra of 1 and 2 keV Ne^+ ions scattered to 40° from the W–Ti thin film surface.

According to the XPS results, the concentration of oxygen at the surface is significantly greater than inside the thin film. In order to determine the origin of oxygen at the surface, the Ne^+ ion scattering experiments has been performed before (spectrum A) and after (spectrum B) the additional pumping by the titanium sublimation pump (TSP) for 1 min. The primary ion energy was 1 keV, and scattering angle was 40°. These two subsequent spectra are presented in Fig. 8. Obviously, the spectrum did not change quantitatively. The peak heights corresponding to oxygen and titanium increased for about 6%, while that corresponding to tungsten increased

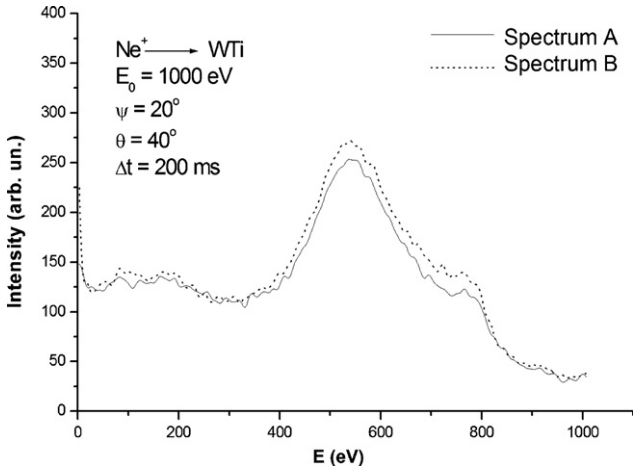

Fig. 8. LEIS spectra of 1 keV Ne^+ ions scattered to 40° from the W–Ti thin film surface; the spectra were measured before and after the system was pumped out by TSP.

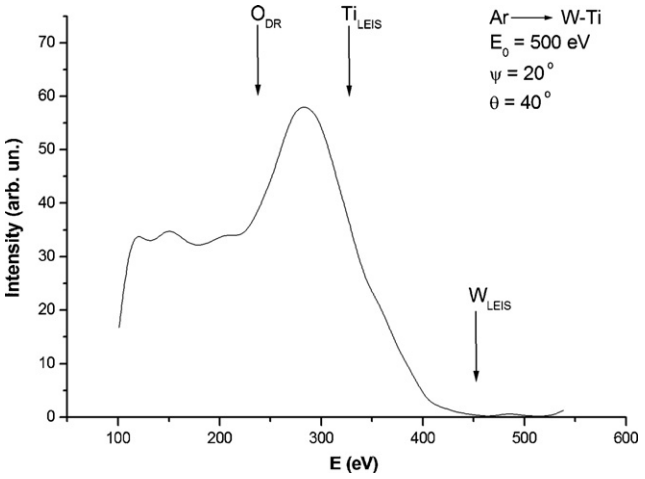

Fig. 9. LEIS spectrum of 500 eV Ar^+ ions scattered to 40° from the W–Ti thin film surface.

for 1% after the use of TSP. Consequently, the oxygen present at the surface is not adsorbed at the surface as an impurity from the residual gas.

The spectrum of Ar^+ ions scattered from the W–Ti thin film surface is presented in Fig. 9. The primary ion energy was 500 eV, and the scattering angle was 40°. One very intense peak can be seen at the position between those corresponding to directly recoiled oxygen and Ar^+ scattered from titanium. Most likely, this peak is a superposition of O_{DR} and Ti_{LEIS} peaks. O_{LEIS} peak does not exist because the single scattering of Ar^+ from oxygen is not possible for this scattering angle. The most important fact concerning this spectrum is absence of the tungsten LEIS peak. Knowing that the information depth in this experiment has been lower than in the other presented LEIS results (the lowest primary ion energy, the greatest atomic number of the projectile), most probably, only titanium and oxygen are present in the first atomic layer.

4. Discussion

The small grain size of the W–Ti thin film is obtained, which is typical for the dc sputtering technique. The possible reason for the increased concentration of tungsten inside the thin film with respect to the target composition according to the XPS measurements could be the preferential sputtering of Ti (which is the lighter component) during the depth profiling in XPS measurements.

The obtained XRD results clearly show significant discrepancy of the W–Ti thin film surface structure and composition as compared to its interior. The observation of TiO_2 crystal phase at the surface by the grazing incidence XRD is directly confirmed by the Ti 2p level shift in XPS spectra. The lateral grain size measured with STM usually agree quite well with the vertical grain size measured with XRD [17,18], which is in contrast to the presented results. This strong discrepancy becomes clear from the XPS results: the metallic thin film is covered by the mix of oxides—TiO_2 and WO_3. LEIS results show however, that oxide overlayer is not homogeneous—the first atomic layer consists of TiO_2 only. WO_3 is not observed in XRD as expected, because this phase is amorphous (i.e. with extremely small grains) unless the sample annealing up to 800 K is performed [19].

Both, LEIS and XPS results show high relative concentration of oxygen in the first few atomic layers of the thin film. The oxygen inside the sample is incorporated as the residual gas during the deposition. The increased concentration of oxygen in the surface layers is most probably due to the sample exposure to the atmosphere after the deposition. The significant increase of the titanium concentration relative to that of tungsten with respect to the thin film interior was observed, just as in AES depth profiles of multilayered metal structures when the surface of the W–Ti film was exposed to air [5]. Moreover, tungsten is not even present in the first atomic layer. On the other hand, surface segregation of the titanium impurity in the tungsten matrix (dilute substitutional solution) is not expected according to the recent theoretical study [20]. The change of the surface composition, as compared to that of the thin film interior, was not observed in the AES depth profiling analysis of the W_xTi_{1-x} a.t. ($x = 0.5$–0.7) thin films either [8]. Hence, the observed surface segregation of titanium is most probably due to the presence of oxygen in the surface layers: from thermodynamics considerations, formation of TiO_2 ($\Delta H_{form} = -944$ kJ/mol) is energetically favored over the formation of WO_3 phase ($\Delta H_{form} = -841.3$ kJ/mol) [21]. The fact that titanium reacted with oxygen (no metallic titanium is found) while tungsten is depleted at the surface confirms this assumption.

5. Conclusion

Concluding the paper, we can say that W–Ti thin films obtained by dc sputtering have significantly different structure and composition of the surface as compared to those of its interior. The major reason is the presence of oxygen in the surface layers due to the sample exposure to the atmosphere after the deposition. Ti concentration increased at the surface and TiO_2 crystalline phase is formed at the surface. On the other hand, the tungsten concentration is significantly decreased and it is even missing in the first atomic layer. The thickness of the TiO_2 layer was estimated to be 3.2 ± 0.4 nm. The obtained results point out that the increased concentration of oxygen is exclusively responsible for the W–Ti composition changes at the W–Ti-metal interface [5].

Acknowledgements

This research was supported by the Ministry of Science and Environmental Protection of the Republic of Serbia, Contract No. 141001, and by the Ministry of Sciences and Technology of the Republic of Slovenia, as a part of bilateral cooperation between Institute of Nuclear Sciences-Vinča and ''Jožef Stefan'' Institute, Ljubljana. We thank to Prof. Dr. Anton Zalar and Dr. Peter Panjan, ''Jožef Stefan'' Institute, Ljubljana, Slovenia, for useful discussions.

References

[1] J.M. Oparowski, R.D. Sisson, R.R. Biederman, Thin Solid Films 153 (1987) 313.
[2] M. Milosavljević, N. Bibić, I.H. Wilson, D. Peruško, Thin Solid Films 164 (1988) 493.
[3] R.S. Nowicki, J.M. Harris, M.A. Nicolet, I.V. Mitchell, Thin Solid Films 53 (1978) 195.
[4] M. Milosavljević, N. Bibić, I.H. Wilson, J. Turković, M. Stojanović, D. Peruško, Advances in Low-temperature Plasma Chemistry, Technology, Applications, vol. 3, Technomic Publishing AG, 1991,, p. 245.
[5] M. Milosavljević, N. Bibić, M. Stojanović, J. Turković, I.H. Wilson, Vacuum 41 (1990) 831.
[6] I. Terzić, N. Bundaleski, Z. Rakočević, N. Oklobdžija, J. Elazar, Rev. Sci. Inst. 7 (2000) 4195.
[7] C. Louro, A. Cavalerro, J. Electrochem. Soc. 144 (1997) 259.
[8] V.G. Glebovsky, V.Yu. Yaschak, V.V. Baranov, E.L. Sackovich, Thin solid films 257 (1995) 1.
[9] S. Petrović, B. Adnadjević, D. Peruško, N. Popović, N. Bundaleski, M. Radović, B. Gaković, Z. Rakočević, J. Serb. Chem. Soc. 71 (2006) 969.
[10] D. Briggs, M.P. Seah, Practical Surface Analyses, Auger and X-ray Photoelectron Spectroscopy, vol. 1, John Wiley and Sons, Chichester, 1994
[11] G.G. Fuentes, E. Elizalde, F. Yubero, J.M. Sanz, Surf. Interf. Anal. 33 (2002) 230.
[12] T.M. Thomas, H. Neumann, A.W. Czanderna, J.R. Pitts, Surf. Sci. 175 (1986) L737.
[13] M. Grundner, W. Heiland, E. Tagaluer, Appl. Phys. 4 (1974) 243.
[14] J.F. Ziegler, J.P. Biersack, U. Littmark, The Stopping and Range of Ions in Solids, Pergamon Press, 1985.
[15] S.N. Mikhailov, R.J.M. Elfrink, J.P. Jacobs, L.C.A. van den Oetelaar, P.J. Scanlon, H.H. Brongersma, Nucl. Instrum. Meth. B 93 (1994) 149.
[16] H. Niehus, W. Heiland, E. Taglauer, Surf. Sci. Rep. 17 (1993) 213.
[17] N. Popović, Ž. Bogdanov, B. Goncić, S. Zec, Z. Rakočević, Thin solid Films 343–344 (1999) 75.
[18] T. Kacsich, M. Neubauer, U. Geyer, K. Baumann, F. Rose, M. Uhrmacher, J. Phys. D: Appl. Phys. 28 (1995) 424.
[19] P. Nelli, L.E. Depero, M. Ferroni, S. Groppelli, V. Guidi, F. Ronconi, L. Sangaletti, G. Sberveglieri, Sens. Actuators B 31 (1996) 89.
[20] L. Vitos, A.V. Ruban, H.L. Skriver, J. Kollar, Surf. Sci. 411 (1998) 186.
[21] Chemical encyclopedia, in: L. Knunyanc (Ed.), Sovietskaya Enciklopediya, Moskva, 1988 (in Russian).